Table 1 Characteristics of subjects at baseline and after the administration of minodronic acid hydrate for 12 months

	Baseline	12 months	*P* value
Age (years)	63.9 ± 6.4	–	–
Body weight (kg)	50.0 ± 6.5	–	–
Body height (cm)	152.3 ± 4.7	–	–
Age at menopause (years)	49.9 ± 3.3	–	–
Lumbar spine BMD (g/cm^2)	0.648 ± 0.051	0.688 ± 0.060	<0.001
Total hip BMD (g/cm^2)	0.635 ± 0.078	0.657 ± 0.077	<0.001
Conventional neck BMD (g/cm^2)	0.542 ± 0.072	0.555 ± 0.070	<0.001
HSA			
Hip axis length (mm)	99.9 ± 5.2	–	–
Neck shaft angle (°)	125.6 ± 5.1	–	–
Bone biomarker			
Urine NTX (nmol BCE/mmol Cr)	53.2 ± 18.6	19.8 ± 9.7	<0.001
Urine total DPD (pmol/mmol Cr)	9.3 ± 2.8	4.5 ± 1.4	<0.001
Serum BALP (U/l)	30.1 ± 10.0	14.6 ± 4.3	<0.001
Serum osteocalcin (ng/ml)	9.3 ± 2.7	4.2 ± 1.0	<0.001

Each value is shown as the mean ± SD

BMD bone mineral density, *HSA* hip structure analysis, *NTX* urine type I collagen N-telopeptide, *DPD* urine total deoxypyridinoline, *BALP* serum bone-specific alkaline phosphatase

All DXA devices were of the Hologic QDR Series, and each machine was adjusted for differences by calibration with standard phantoms to verify the reproducibility of the measurements within ±1.5% during the study period. DXA image data for the proximal femur were analyzed using the HSA program (Version 12.7.3.1), and all analyses were conducted by the same technician (T.T.) in the Department of Nuclear Medicine, Kawasaki Medical School.

The HSA algorithm is based on a principle first articulated by Martin and Burr [14], who demonstrated that mineral profiles created during a single photon absorptiometry bone density scan are a projection of the corresponding bone cross section and can be used to define its geometry. As described previously [2, 15, 16], the HSA algorithm derives the conventional BMD (g/cm^2), the outer diameter (OD, cm), the endocortical diameter (ED, cm), the average cortical thickness (CoTh, cm), the total mineralized bone area in the cross section (CSA, cm^2), the cross-sectional moment of inertia (CSMI, cm^4), and the section modulus (SM, cm^3) directly from the mass profiles. SM is computed as CSMI/d_{max}, where d_{max} (cm) is the maximum distance between the center of the mass (centroid) and the outer cortex. Another parameter, the buckling ratio (BR), is estimated as the ratio of d_{max} to the estimated average CoTh derived from an annulus model of the cross section using the measured OD, assuming that a fixed proportion of CSA is in the cortex. CSA and SM are indices of resistance to axial compressive and bending loads, respectively, and BR is an index of susceptibility to local buckling under bending loads.

The HSA software generates profiles of pixel values traversing the proximal femur at three locations: the narrow neck (NN) across the femoral neck at its narrowest point, the intertrochanter (IT) along the angle bisector defined by the neck and shaft axes, and across the shaft at 30 mm below the most prominent portion of the lesser trochanter. To avoid variation in the visualization of the lower border of the lesser trochanter depending on the inner rotation of the hip joint, the distance from the highest part of the lesser trochanter was made constant to improve the reproducibility of bone shaft regions and to correctly determine the region of interest (ROI). At each of these locations, five parallel profiles were generated, spaced one pixel apart, proximal and distal to the three defined locations. The five profiles were averaged within each region, and the BMD, CSA, OD, ED, CoTh, CSMI, SM, and BR were reported. The reproducibility of the HSA parameters was calculated using two measurements at a 1- or 2-month interval from 30 women [age 56–86 years old (range 71.8 ± 7.6 years)] (Table 2).

Table 2 Reproducibility of HSA parameters in the three regions

	CV (%)		
	Neck	Trochanter	Shaft
Cross-sectional area	1.91	2.88	1.72
Subperiosteal width	2.15	1.40	0.65
Endocortical width	2.47	1.53	1.63
Cortical thickness	3.87	3.11	2.31
CSMI	6.10	4.80	2.17
Section modulus	3.50	4.11	1.81
Buckling ratio	5.54	3.11	2.74

The reproducibility was calculated using two measurements at 1- or 2-month intervals from 30 women

CV coefficient of variation, *HSA* hip structure analysis, *CSMI* cross-sectional moment of inertia

Statistical analysis

For each case, the change (%) from baseline was calculated for each parameter, and summary statistics were obtained at individual time points. These data are expressed as average values and standard deviations (SD). Comparison of the findings before and after administration of minodronic acid hydrate was performed by Wilcoxon test, assuming a two-sided level of significance of 5% ($P < 0.05$).

Results

Changes in BMD from baseline

Percentage changes in BMD of individual femoral regions from baseline are shown in Fig. 1. The BMD significantly increased in all regions after 3–6 months administration of minodronic acid hydrate and increased by 3.2% ($P < 0.001$), 4.1% ($P < 0.001$), and 1.6% ($P < 0.001$) in the NN, IT, and shaft, respectively, after 12 months. The largest change was observed in the trochanteric region. The femoral BMD, geometry, and bone strength indices at baseline and 12 months are shown in Table 3.

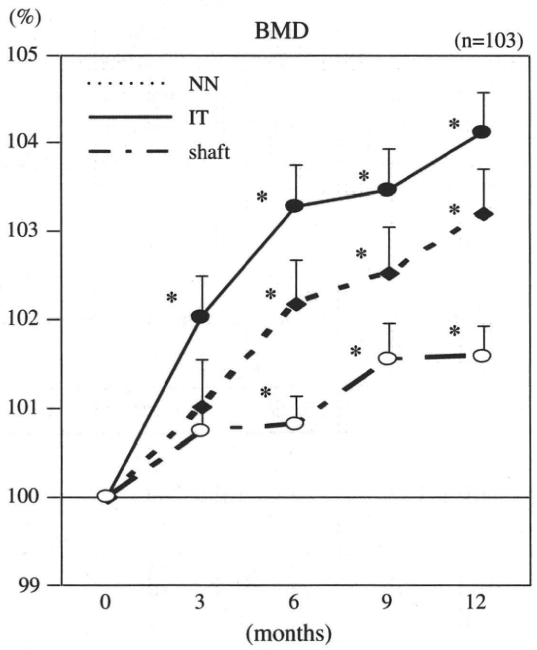

Fig. 1 Percentage changes from baseline of bone mineral density (*BMD*) in the femoral neck, trochanter, and shaft at 3, 6, 9, and 12 months of treatment. Data are shown as means ± SE ($n = 103$); *$P < 0.05$ versus baseline (Wilcoxon test). *NN* narrow neck, *IT* intertrochanter

Changes in bone geometry from baseline

Percentage changes in bone geometry from baseline are shown in Fig. 2. CSA significantly increased in all the femoral regions starting 3 months after administration and increased by 3.3% ($P < 0.001$), 3.9% ($P < 0.001$), and 2.0% ($P < 0.001$) in the NN, IT, and shaft after 12 months. The changes in OD from baseline were 0.1, −0.2, and 0.4% in the NN, IT, and shaft, respectively, at 12 months after administration, with none of these changes reaching a significant level, except for OD in the shaft at 12 months ($P = 0.015$). ED deceased from baseline by −0.1, −0.6, and −0.2% in the NN, IT, and shaft, respectively, after 12 months, showing a trend for a decrease but without significance in any region. CoTh significantly increased from baseline at 3 months after administration and increased by 3.1% ($P < 0.001$), 3.7% ($P < 0.001$), and 2.0% ($P < 0.001$) in the NN, IT, and shaft, respectively, after 12 months. Overall, the most significant changes were observed in IT.

Changes in bone strength indices from baseline

Percentage changes from baseline in CSMI, SM, and BR, all of which are bone strength indices for the femoral region, are shown in Fig. 3. CSMI and SM showed significant increases in all the femoral regions examined 3 months after administration; CSMI increased by 4.8% ($P < 0.001$), 4.9% ($P < 0.001$), and 3.2% ($P < 0.001$) and SM by 4.9% ($P < 0.001$), 5.8% ($P < 0.001$), and 2.9% ($P < 0.001$) in the NN, IT, and shaft, respectively, after 12 months. BR significantly decreased at 3 months after administration in the IT and at 6 months after administration in the NN and shaft. BR significantly decreased by −3.0% ($P < 0.001$), −4.2% ($P < 0.001$), and −1.4% ($P = 0.028$) in the NN, IT, and shaft, respectively, after 12 months.

As seen for BMD and the geometry indices, the effects of minodronic acid hydrate on the bone strength indices most significantly appeared in the IT, followed by the NN, and then the shaft.

Discussion

The present study demonstrates that minodronic acid hydrate, a new bisphosphonate, improves bone strength indices in the proximal femur in patients with osteoporosis. The comparison of femoral geometry and bone strength indices before and after administration allows investigation of the mechanism of drug action in the prevention of fracture. Specifically, most changes in the indices for bone density, geometry, and strength were observed in all

Table 3 Femoral BMD, geometry, and strength indices at baseline and after the administration of minodronic acid hydrate for 12 months

	Baseline	12 months	*P* value
Narrow neck (NN)			
BMD (g/cm^2)	0.661 ± 0.091	0.681 ± 0.092	<0.001
CSA (cm^2)	1.933 ± 0.237	1.993 ± 0.229	<0.001
Outer diameter (OD) (cm)	3.085 ± 0.231	3.088 ± 0.231	0.812
Endocortical diameter (ED) (cm)	2.834 ± 0.250	2.829 ± 0.253	0.345
Cortical thickness (CoTh) (cm)	0.126 ± 0.018	0.130 ± 0.019	<0.001
CSMI (cm^4)	1.585 ± 0.337	1.650 ± 0.327	<0.001
Section modulus (SM) (cm^3)	0.899 ± 0.154	0.937 ± 0.141	<0.001
Buckling ratio (BR)	14.389 ± 2.895	13.922 ± 2.874	<0.001
Intertrochanter (IT)			
BMD (g/cm^2)	0.639 ± 0.099	0.664 ± 0.098	<0.001
CSA (cm^2)	3.135 ± 0.488	3.250 ± 0.485	<0.001
Outer diameter (OD) (cm)	5.162 ± 0.310	5.150 ± 0.307	0.672
Endocortical diameter (ED) (cm)	4.612 ± 0.331	4.581 ± 0.329	0.096
Cortical thickness (CoTh) (cm)	0.275 ± 0.044	0.284 ± 0.046	<0.001
CSMI (cm^4)	7.718 ± 1.811	8.047 ± 1.798	<0.001
Section modulus (SM) (cm^3)	2.520 ± 0.531	2.652 ± 0.525	<0.001
Buckling ratio (BR)	11.464 ± 2.327	10.956 ± 2.172	<0.001
Shaft			
BMD (g/cm^2)	1.204 ± 0.149	1.222 ± 0.150	<0.001
CSA (cm^2)	3.080 ± 0.362	3.141 ± 0.370	<0.001
Outer diameter (OD) (cm)	2.697 ± 0.200	2.709 ± 0.205	0.014
Endocortical diameter (ED) (cm)	1.817 ± 0.297	1.813 ± 0.304	0.745
Cortical thickness (CoTh) (cm)	0.440 ± 0.072	0.448 ± 0.072	<0.001
CSMI (cm^4)	2.209 ± 0.473	2.278 ± 0.492	<0.001
Section modulus (SM) (cm^3)	1.570 ± 0.244	1.616 ± 0.255	<0.001
Buckling ratio (BR)	3.278 ± 0.694	3.228 ± 0.693	0.026

Each value is shown as the mean ± SD

BMD bone mineral density, *HSA* hip structure analysis, *CSMI* cross-sectional moment of inertia

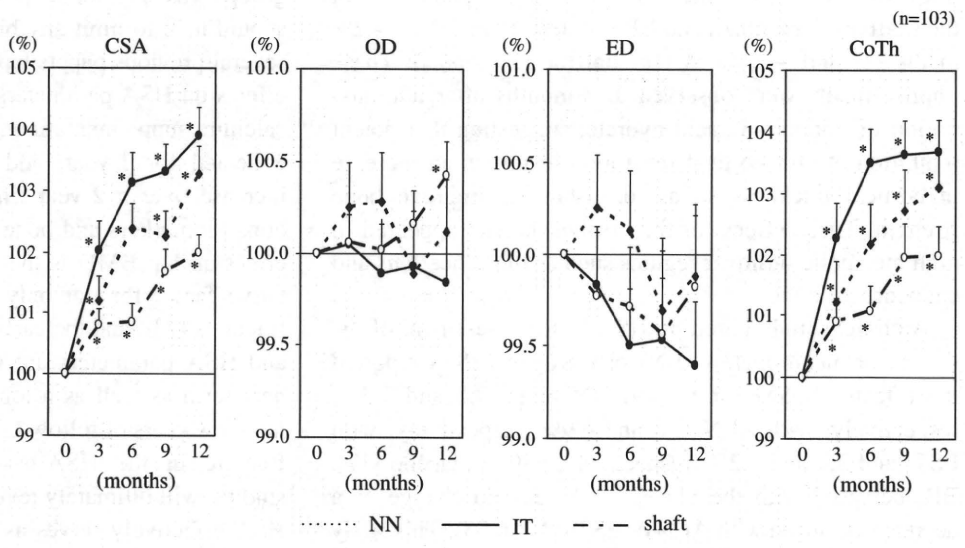

Fig. 2 Percentage changes from baseline of the cross-sectional area, outer and endocortical diameters, and cortical thickness of the femoral head, trochanter, and shaft at 3, 6, 9, and 12 months of treatment. Data are shown as means ± SE ($n = 103$); *$P < 0.05$ versus baseline (Wilcoxon test). *CSA* cross-sectional area, *OD* outer diameter, *ED* endocortical diameter, *CoTh* cortical thickness, *NN* narrow neck, *IT* intertrochanter

femoral regions starting from an early stage (3–6 months) after administration of minodronic acid hydrate. The strongest effect occurred in the femoral trochanteric region as a result of the dominant action of the bisphosphonate on cancellous bone. No significant increase in the outer diameter, which is reported to typically occur with aging, was observed during the 12-month follow-up period; in contrast, it is of interest that a slight decrease in

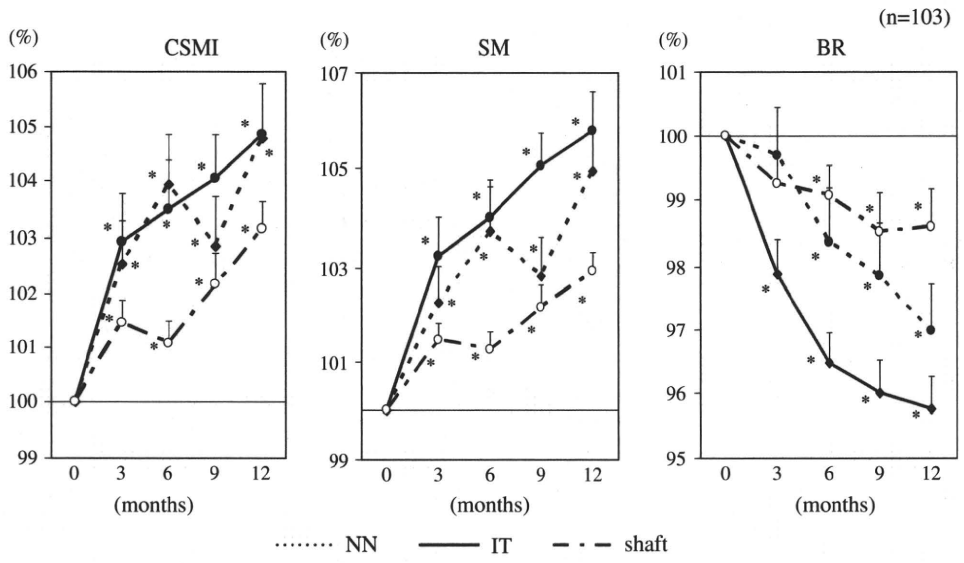

Fig. 3 Percentage changes from baseline of bone strength indices (CSMI, SM, BR) of the femoral neck, trochanter, and shaft at 3, 6, 9, and 12 months of treatment. Data are shown as means ± SE ($n = 103$); *$P < 0.05$ versus baseline (Wilcoxon test). *CSMI* cross-sectional moment of inertia, *SM* section modulus, *BR* buckling ratio, *NN* narrow neck, *IT* intertrochanter

endocortical diameter (−0.1% in the NN, −0.6% in the IT, and −0.2% in the shaft) was observed, which is generally thought to increase with aging. This change might be caused by an inhibition of endocortical resorption by minodronic acid hydrate, resulting in a significantly increased CSA (3.3% in the NN, 3.9% in the IT, and 2.0% in the shaft) and CoTh (3.1% in the NN, 3.7% in the IT, and 2.0% in the shaft). The bone strength parameters calculated by the HSA algorithm include the cortical CSA as an index of strength against axial compressive load, CSMI and SM as strength indices against bending load, and BR as an index for predisposition to local buckling caused by thinned cortices. In the present study, we found a significant change in CSMI, SM (4.9% in the NN, 5.8% in the IT, and 2.9% in the shaft at 12 months), and BR (−3.0% in the NN, −4.2% in the IT, and −1.4% in the shaft at 12 months). These improvements were observed at 3 months after administration of minodronic acid hydrate, suggesting that potent inhibition of endocortical resorption results in an increase in cortical thickness so as to sustain or improve bone strength. These effects of the bisphosphonate appeared in high metabolic turnover regions such as the cancellous and endocortical bone.

A clinical study based on HSA-based assessment of the effects of alendronate (ALN) or estrogen (EST) reported the effects on SM for IT and NN to be 9.1 and 7.3%, respectively, with ALN; 5.8 and 6.9%, respectively, with EST; and 3.4 and 3.2%, respectively, with a placebo [17]. BR increased with the placebo, whereas no change or a decrease occurred with ALN or EST ($P < 0.05$). This study was performed in 373 women over the age of 65 years for 3 years. In the Fosamax Actonel Comparison Trial (FACT study), ALN and risedronate (RIS) were administered once weekly (70 and 35 mg/week, respectively) for 2 years, and HSA-based assessment showed that both bisphosphonates improved bone geometry [18]. ALN and RIS increased SM by 6–7% and approximately 4%, respectively, while ALN decreased BR by approximately 2% and RIS increased BR by approximately 1% in the narrow neck. It is difficult to compare the results in the present study with previous studies on bisphosphonates because of differences in the race and age of the subjects, the criteria for diagnosis of osteoporosis in patients with low bone density, and dose and administration method (daily or weekly). However, prominent effects of minodronic acid hydrate were observed that were similar to those reported for other bisphosphonates.

The current study has the limitation that no control group was included; however, the multicenter design should help to limit any bias in the findings. Furthermore, several previous papers have reported there are no positive effects on HSA parameters in the placebo group receiving calcium supplementation at 1 year [19–22]. Data were collected for 1 year, and the effects of the agent may increase over a 2-year time-course based on changes in bone biomarkers and bone density [10, 11]. The beneficial effect on hip BMD is thought to be an important preventative factor for not only hip fracture but also vertebral fractures [23], and the early significant effects on hip BMD and HSA parameters are thought to be important for the near term as well as a longer-term preventive effect. The next few years of follow-up, to observe the incidence of hip fracture in the HSA-based assessment of intervention studies, will ultimately reveal whether geometry derived by HSA effectively serves as a surrogate marker of hip fracture. In fact, a review of reports using HSA in evaluation of the efficacy of antiosteoporotic agents [17–22] suggests that potent increase in bone strength indices derived from HSA does have an association with reduction in the incidence of hip fracture [24–26].

Previous HSA-based studies of bisphosphonate effects on the proximal femur have only included Caucasian patients. As there may be a racial difference in hip geometry, bone size, and bone density, HSA results might differ among races. Only one study using HSA assessment in Japanese patients has been performed to investigate the effects of an antiosteoporotic agent (raloxifene) [27], and therefore our study provides the first multicenter evidence of the efficacy of a bisphosphonate on hip geometry in a Japanese population. We conclude that minodronic acid hydrate may prevent hip fracture by inhibiting aging-related endocortical resorption, resulting in increased cortical thickness and improved bone strength indices in the proximal femoral region.

Acknowledgments We express our gratitude to Dr. Tatsushi Tomomitsu, the Department of Nuclear Medicine, Kawasaki Medical School, for his help with the HSA-based assessment. Pacific Edit reviewed the manuscript before submission.

References

1. Yoshikawa T, Turner CH, Peacock M, Slemenda CW, Weaver CM, Teegarden D, Markwardt P, Burr DB (1994) Geometric structure of the femoral neck measured using dual-energy X-ray absorptiometry. J Bone Miner Res 9:1053–1064
2. Beck TJ, Ruff CB, Warden KE, Scott WW Jr, Rao GU (1990) Predicting femoral neck strength from bone mineral data. A structural approach. Invest Radiol 25:6–18
3. Ahlborg HG, Nguyen ND, Nguyen TV, Center JR, Eisman JA (2005) Contribution of hip strength indices to hip fracture risk in elderly men and women. J Bone Miner Res 20:1820–1827
4. Rivadeneira F, Zillikens MC, De Leat CE, Hofman A, Uitterlinden AG, Beck TJ, Pols HA (2007) Femoral neck BMD is a strong predictor of hip fracture susceptibility in elderly men and women because it detects cortical bone instability: the Rotterdam study. J Bone Miner Res 22:1781–1790
5. Kaptoge S, Beck TJ, Reeve J, Stone KL, Hiller TA, Cauley JA, Cummings SR (2008) Prediction of incident hip fracture risk by femur geometry variables measured by hip structural analysis in the study of osteoporotic fractures. J Bone Miner Res 23:1892–1904
6. Mayhew P, Kaptoge S, Loveridge N, Power J, Kroger HP, Parker M, Reeve J (2004) Discrimination between cases of hip fracture and controls is improved by hip structural analysis compared to areal bone mineral density. An ex vivo study of the femoral neck. Bone (NY) 34:352–361
7. Mori H, Kayasuga R, Tanaka M, Kawabata K, Nozaki K, Mori M, Sasamata M (2008) Inhibitory effect of minodronic acid on bone resorption in vitro and in vivo. Clin Pharmacol Ther 18:S19–S32
8. Tanaka M, Mori H, Kayasuga R, Ochi Y, Kawada N, Yamada H, Kishikawa K (2008) Long-term minodronic acid (ONO-5920/YM529) treatment suppresses increased bone turnover, plus prevents reduction in bone mass and bone strength in ovariectomized rats with established osteopenia. Bone (NY) 43:894–900
9. Mori H, Tanaka M, Kayasuga R, Masuda T, Ochi Y, Yamada H, Kishikawa K, Ito M, Nakamura T (2008) Minodronic acid (ONO-5920/YM529) prevents decrease in bone mineral density and bone strength, and improves bone microarchitecture in ovariectomized cynomolgus monkeys. Bone (NY) 43:840–848
10. Hagino H, Nishizawa Y, Sone T, Morii H, Taketani Y, Nakamura T, Itabashi A, Mizunuma H, Ohashi Y, Shiraki M, Minamide T, Matsumoto T (2009) A double-blinded head-to-head trial of minodronate and alendronate in women with postmenopausal osteoporosis. Bone (NY) 44:1078–1084
11. Matsumoto T, Hagino H, Shiraki M, Fukunaga M, Nakano T, Takaoka K, Morii H, Ohashi Y, Nakamura T (2009) Effect of daily oral minodronate on vertebral fractures in Japanese postmenopausal women with established osteoporosis: a randomized placebo-controlled double-blind study. Osteoporos Int 20(8):1429–1437
12. Orimo H, Sugioka Y, Fukunaga M, Muto Y, Hotokebuchi T, Gorai I, Nakamura T, Kushida K, Tanaka H, Ikai T, Oh-hashi Y, The Committee of the Japanese Society for Bone and Mineral Research for Development of Diagnosis Criteria of Osteoporosis (1998) Diagnostic criteria of primary osteoporosis. J Bone Miner Metab 16:139–150
13. Orimo H, Hayashi Y, Fukunaga M, Sone T, Fujiwara S, Shiraki M, Kushida K, Miyamoto S, Soen S, Nishimura J, Oh-Hashi Y, Hosoi T, Gorai I, Tanaka H, Igai T, Kishimoto H, Osteoporosis Diagnostic Criteria Review Committee: Japanese Society for Bone and Mineral Research (2001) Diagnostic criteria for primary osteoporosis: year 2000 revision. J Bone Miner Metab 19:331–337
14. Martin RB, Burr DB (1984) Non-invasive measurement of long bone cross-sectional moment of inertia by photon absorptiometry. J Biomech 17:195–201
15. Beck TJ (2007) Extending DXA beyond bone mineral density: understanding hip structure analysis. Curr Osteoporos Rep 5:49–55
16. Beck T (2003) Measuring the structural strength of bones with dual-energy X-ray absorptiometry: principles, technical limitations, and future possibilities. Osteoporos Int 14:S81–S88
17. Greenspan SL, Beck TJ, Resnick NM, Bhattacharya R, Parker RA (2005) Effect of hormone replacement, alendronate, or combination therapy on hip structural geometry: a 3-year, double-blind, placebo-controlled clinical trial. J Bone Miner Res 20:1525–1532
18. Bonnick SL, Beck TJ, Cosman F, Hochberg MC, Wang H, de Papp AE (2009) DXA-based hip structural analysis of once-weekly bisphosphonate-treated postmenopausal women with low bone mass. Osteoporos Int 20:911–921
19. Beck TJ, Stone KL, Oreskovic TL, Hochberg MC, Nevitt MC, Genant HK, Cummings SR (2001) Effects of current and discontinued estrogen replacement therapy on hip structural geometry: the study of osteoporotic fractures. J Bone Miner Res 16:2103–2110
20. Uusi-Rasi K, Semanick LM, Zanchetta JR, Bogado CE, Eriksen EF, Sato M, Beck TJ (2005) Effects of teriparatide [rhPTH (1–34)] treatment on structural geometry of the proximal femur in elderly osteoporotic women. Bone (NY) 36:948–958
21. Uusi-Rasi K, Beck TJ, Semanick LM, Daphtary MM, Crans GG, Desaiah D, Harper KD (2006) Structural effects of raloxifene on the proximal femur: results from the multiple outcomes of raloxifene evaluation trial. Osteoporos Int 17:575–586
22. Beck TJ, Lewiecki EM, Miller PD, Felsenberg D, Liu Y, Ding B, Libanati C (2008) Effects of denosumab on the geometry of the proximal femur in postmenopausal women in comparison with alendronate. J Clin Densitom 11:351–359
23. Bauer DC, Black DM, Garnero P, Hochberg M, Ott S, Orloff J, Thompson DE, Ewing SK, Delmas PD, for the Fracture Intervention Trial Study Group (2004) Change in bone turnover and hip, non-spine, and vertebral fracture in alendronate-treated women: the Fracture Intervention Trial. J Bone Miner Res 19:1250–1258
24. Black DM, Thompson DE, Bauer DC, Ensrud K, Musliner T, Hochberg MC, Nevitt MC, Suryawanshi S, Cummings SR,

Fracture Intervention Trial (2000) Fracture risk reduction with alendronate in women with osteoporosis: the Fracture Intervention Trial. FIT Research Group. J Clin Endocrinol Metab 85:4118–4124

25. Black DM, Cummings SR, Karpf DB, Cauley JA, Thompson DE, Nevitt MC, Bauer DC, Genant HK, Haskell WL, Marcus R, Ott SM, Torner JC, Quandt SA, Reiss TF, Ensrud KE (1996) Randomised trial of effect of alendronate on risk of fracture in women with existing vertebral fractures. Fracture Intervention Trial Research Group. Lancet 348:1535–1541
26. McClung MR, Geusens P, Miller PD, Zippel H, Bensen WG, Roux C, Adami S, Fogelman I, Diamond T, Eastell R, Meunier PJ, Reginster JY, Hip Intervention Program Study Group (2001) Effect of risedronate on the risk of hip fracture in elderly women. Hip Intervention Program Study Group. N Engl J Med 344:333–340
27. Takada J, Beck TJ, Miki T, Imanishi Y, Nakatsuka K, Wada H, Naka H, Iba K, Yoshizaki T, Yamashita T (2008) Hip structure analysis for raloxifene treatment in Japanese women with osteoporosis. J Bone Miner Res 23(Suppl 1):S211

Bone 48 (2011) 627–630

Contents lists available at ScienceDirect

Bone

journal homepage: www.elsevier.com/locate/bone

Age-related changes in bone density, geometry and biomechanical properties of the proximal femur: CT-based 3D hip structure analysis in normal postmenopausal women

Masako Ito [a,b,*], Tomoko Nakata [b], Akifumi Nishida [a], Masataka Uetani [a]

[a] Department of Radiology, Nagasaki University School of Medicine, 1-7-1 Sakamoto, Nagasaki 852-8501, Japan
[b] Division of Radiology, Nagasaki University Hospital, Nagasaki, Japan

ARTICLE INFO

Article history:
Received 24 September 2010
Revised 5 November 2010
Accepted 9 November 2010
Available online 16 November 2010

Edited by: Toshio Matsumoto

Keywords:
Hip geometry
Bone mineral density (BMD)
Computed tomography (CT)
Osteoporosis

ABSTRACT

The geometry as well as bone mineral density (BMD) of the proximal femur contributes to fracture risk. How and the extent to which they change due to natural aging is not fully understood.
We assessed BMD and geometry in the femoral neck and shaft separately, in 59 normal Japanese postmenopausal women aged 54–84 years, using clinical computed tomography (CT) and commercially available software, at baseline and 2-year follow-up. This system detected significant reductions over the 2-year interval in total BMD (%change/year = -0.900 ± 0.257, $p<0.0005$), cortical cross-sectional area (CSA) (-0.800 ± 0.423%/year, $p<0.05$) and cortical thickness (-1.120 ± 0.453%/year, $p<0.01$) in the femoral neck. In the femoral shaft, cortical BMD decreased significantly (-0.642 ± 0.188%/year, $p<0.005$). Regarding biomechanical parameters in the femoral neck, the cross-sectional moment of inertia (CSMI) and section modulus (SM) decreased (-1.38 ± 3.65%/year, $p<0.01$ and -1.37 ± 2.96%/year, $p<0.005$) and the buckling ratio (BR) increased significantly (1.48 ± 4.81%/year, $p<0.05$), whereas no changes were found in the femoral shaft.
The distinct patterns of age-related changes in the geometry and biomechanical properties in the femoral neck and shaft suggest that improved geometric measures are possible with the current non-invasive method using clinical CT.

© 2010 Elsevier Inc. All rights reserved.

Introduction

The incidence of vertebral fracture increases linearly with aging and correlates closely with a decline in spinal bone mineral density (BMD). The incidence of hip fracture, on the other hand, increases exponentially with advancing age, although hip BMD decreases linearly, suggesting that age-related factors other than BMD contribute substantially to the fragility of the proximal femur. Declining BMD and geometry of the proximal femur, as well as an increase in the incidence of fall are believed to underlie the increased risk of hip fracture in the elderly [1–3]. Non-invasive techniques can provide bone structural information, beyond simple bone densitometry, to help assess fracture risk.

The aging skeleton is characterized by a deterioration of the trabecular microstructure, increased endocortical bone resorption, decreased cortical bone density or increased cortical porosity, and increased periosteal bone formation [4]. In postmenopausal women, the rate of periosteal bone formation declines to a greater extent, while endosteal bone resorption is more elevated, compared with age-matched men. However, the natural course of these cortical changes with aging has not been well elucidated, and how faithfully non-invasive methods can detect these changes over time is also unknown.

Age-related changes in the cortical bone of the femoral neck as well as the shaft have been investigated by means of histology or computed tomography (CT) images. Although cross-sectional analyses of age-related changes in hip geometry have been reported using clinical CT [5,6] or dual X-ray absortiometry (DXA) [7], there have been no reports of age-related changes in geometry along with BMD in the femoral neck and shaft simultaneously, and which also followed the changes longitudinally in the same subjects.

Here we report the results of longitudinal as well as cross-sectional analyses of clinical CT on age-related changes in BMD, geometry and biomechanical properties of the proximal femur, neck and shaft separately, in the same cohort of healthy postmenopausal Japanese women. The information provided in this study may form the basis for future investigation into how osteoporosis intervention impacts the biomechanical properties along with the structure of the femoral neck and shaft.

* Corresponding author. Department of Radiology, Nagasaki University School of Medicine, 1-7-1 Sakamoto, Nagasaki 852-8501, Japan. Fax: +81 95 819 7357.
E-mail address: masako@nagasaki-u.ac.jp (M. Ito).

8756-3282/$ – see front matter © 2010 Elsevier Inc. All rights reserved.
doi:10.1016/j.bone.2010.11.007

Subjects and methods

Subjects

The subjects were 59 postmenopausal women who had volunteered to have spinal BMD measurements taken annually by DXA [8] and agreed to participate in the current prospective CT study. They were aged 54–84 (67.0 ± 7.4) years of age and had no physical problems in daily life. Their BMD values in the lumbar spine and the proximal femur were above 70% of the Japanese young adult mean [9]. None of the participants had any prevalent radiological vertebral fracture based on the semi-quantitative method of Genant [10], or any history of fragility fractures of hip, radius and humerus. They were enrolled in hip CT studies in August 2006 or December 2006 at the baseline and in August 2008 or December 2008 for the follow-up study. Table 1 summarizes their demographic features.

The study was reviewed and approved by the appropriate Internal Review Boards at Nagasaki University Hospital. Written informed consent to participate was obtained from all subjects.

CT data acquisition

A multi-detector-row CT (MDCT) scanner (Aquilion16, Toshiba Medical Systems Corporation, Tokyo, Japan) at Nagasaki University Hospital was used, and the same X-ray scan conditions, including kVp, mAs and beam pitch, were employed for the baseline and follow-up studies. The average number of slices was 690 ± 33.3. CT scanning of the proximal femur was performed twice during a 2-year period (1.99 ± 0.01 years). The reference phantom which was scanned simultaneously, was a B-MAS200 (Fujirebio Inc., Japan) containing hydroxyapatite at 0, 50, 100, 150 and 200 mg/cm^3. The scanning conditions were adjusted to 120 kV, 250 mA and a reconstruction thickness of 0.5 mm, and the spatial resolution was 0.625 × 0.625 mm. The radiation dose was 19.7 mGy at maximum, as shown by the CTDIvol [3].

The subjects were scanned in the supine position, with the reference phantom placed under them so as to cover a region from the top of the acetabulum to 5 cm below the bottom of the lesser trochanter in both hip joints. A bolus bag was placed between the subject and the CT calibration phantom. The CT scanner table height was set to the center of the greater trochanter.

Analysis of BMD and geometry data obtained by CT

The BMD and geometry data of the proximal femur were analyzed by a radiologist (M.I.), using commercial software (QCT PRO; Mindways, Austin, USA). The exact 3-D rotation of the femur and the threshold setting for defining the bone contours appeared to be the two most critical steps to ensure the accuracy and reproducibility of the automated procedure. The femoral neck axis was identified visually and automatically with the "Optimize FN Axis" algorithm. The CT values were converted to BMD scale using a solid reference phantom. QCT BIT processing was then performed with a fixed bone threshold for inner cortical separation, which was set to 350 mg/cm^3 for all of the CT images.

The BMD and the areas (CSA) of total and cortical regions of the cross-sectional femoral neck, as well as cortical thickness and the cortical perimeter, were calculated using QCT PRO software. Trabecular BMD and CSA were calculated on the basis of the total and cortical BMD and CSA. Cortical thickness was measured as the average of the whole cortex [11]. In the cross-sectional femoral shaft, the cortical BMD, CSA and perimeter were determined. As biomechanical parameters, the cross-sectional moment of inertia (CSMI), section modulus (SM) and buckling ratio (BR) were obtained for the femoral neck, and CSMI and SM for the femoral shaft. SM is a parameter calculated as the CSMI divided by the distance to the center of mass (CM) (d_{max}). BR was calculated as the d_{max} divided by the average cortical thickness in this study. They are derived in a manner intended to be consistent with the DXA-based HSA method implemented by Tom Beck [12].

The reproducibility (% coefficient of variation) of the analysis by the QCT PRO program was calculated using five repeated analyses with visual matching each time from seven healthy subject CT data sets from this study without visible artifact; coefficient of variation (%) as the root mean square standard deviation divided by the mean, for the total BMD was 1.49%, cortical BMD 2.63%, total mass 1.12%, total area 1.71%, cortical area 2.11%, cortical perimeter 2.11%, and cortical thickness 3.58% for FN. In the femoral shaft, the CV% was 0.52% for cortical BMD, 0.77% for cortical CSA, 1.10% for perimeter, 2.19% for CSMI and 1.00% for SM.

The high correlation ($r = 0.84$ to 0.98; $p < 0.0001$ in all) between the baseline and follow-up measurements (shown in Table 3) indicates the high reproducibility of the measurements using clinical CT and of the analysis performed by this application.

Statistical analysis

In the cross-sectional study, we calculated a linear regression as a function of age, and the correlation coefficients (r). In the longitudinal study, the follow-up data was compared with the baseline data using t-test, and also for each case, the average percent (%) changes of the follow-up data from the baseline were calculated, and the data obtained in the femoral neck and the femoral shaft were compared using t-test. These are expressed as average values (mean) and standard deviations (SD), assuming a two-sided level of significance of 5% ($p < 0.05$). These analyses were performed using SPSS version 11.

Results

Correlation between age and BMD/geometry/biomechanical properties at the baseline

Table 1 summarizes the demographic features of the 59 participants. They were healthy postmenopausal Japanese women who volunteered this study, and their ages ranged over 30 years, from 54 to 84 (67.0 ± 7.4) years. They did not have any fractures or a diagnosis of osteoporosis according to the BMD criteria of Japanese Society for Bone and Mineral Research (JSBMR) [9]. As a first step to obtaining information on the natural course of structural changes with advancing age, we examined if there were any correlations between the ages of the subjects and BMD/geometry/biomechanical properties of the proximal femur at baseline.

As shown in Table 2, at the femoral neck, the total BMD (−3.07 g/cm^3/year; $r = 0.39$, $p < 0.005$) and total bone mass (−0.019 g/year; $r = 0.47$, $p < 0.0005$) negatively correlated with age, while total CSA exhibited no correlation (0.008 cm^2/year; $r = 0.08$, ns). Cortical CSA (−0.028 cm^2/year; $r = 0.51$, $p < 0.0001$), cortical bone mass (−0.019 g/year; $r = 0.46$, $p < 0.0005$) and cortical thickness (−0.025 mm/year; $r = 0.46$, $p < 0.0005$) also negatively correlated with age, while cortical BMD exhibited no

Table 1
Demographics of participants.

		Mean	SD
Age	years	67.0	7.4
Body weight	kg	54.7	14.2
Body height	cm	150.2	14.3
Age at menopause	years	50.4	4.1
Femoral neck BMD	g/cm^2	0.752	0.095
T-score	1	−1.2	0.8
Z-score	1	0.8	0.7

BMD, bone mineral density measured by DXA.

Table 2
Correlations between age and BMD, geometry and biomechanical properties at the baseline.

Measurement		Change/year	Unit	r	p
FN BMD/geometry					
Total BMD		−3.065	mg/cm^3/year	0.39	<0.005
Total CSA		0.008	cm^2/year	0.08	ns
Total bone mass		−0.019	g/year	0.47	<0.0005
Cortical BMD		−0.997	mg/cm^3/year	0.15	ns
Cortical CSA		−0.028	cm^2/year	0.51	<0.0001
Cortical bone mass		−0.019	g/year	0.46	<0.0005
Cortical thickness		−0.025	mm/year	0.46	<0.0005
Perimeter		0.014	mm/year	0.23	<0.05
FS BMD/geometry					
Cortical BMD		−1.965	mg/cm^3/year	0.29	<0.01
Cortical bone area		−0.011	cm^2/year	0.26	<0.05
Perimeter		0.007	mm/year	0.10	ns
Biomechanical property					
FN	CSMI	−0.008	cm^4/year	0.37	<0.005
	SM	−0.006	cm^3/year	0.41	<0.005
	BR	0.104	1/year	0.51	<0.0001
FS	CSMI	−0.005	cm^4/year	0.17	ns
	SM	−0.005	cm^3/year	0.28	<0.05

FN, femoral neck; FS; femoral shaft; BMD, bone mineral density; CSA, cross-sectional area; CSMI, cross-sectional moment of inertia; SM, section modulus; BR, buckling ratio.

correlation (−0.997 mg/cm^3/year; $r=0.15$, ns). The bone perimeter exhibited a positive correlation with age (0.014 mm/year; $r=0.23$, $p<0.05$).

At the femoral shaft, cortical BMD (−1.965 mg/cm^3/year; $r=0.29$, $p<0.001$) and cortical CSA (−0.011 cm^2/year; $r=0.26$, $p<0.05$) negatively correlated with age, while the bone perimeter did not exhibit any correlation.

Regarding the biomechanical properties shown in Table 2, CSMI (−0.008 cm^4/year; $r=0.37$, $p<0.005$) and SM (−0.006 cm^3/year; $r=0.41$, $p<0.005$) at the femoral neck exhibited a significant negative correlation with age. These changes were smaller at the femoral shaft (−0.005 cm^4/year; $r=0.17$, ns for CSMI, −0.005 cm^3/year; $r=0.28$, $p<0.05$ for SM). BR at the femoral neck displayed a positive correlation with age (0.104/year; $r=0.51$, $p<0.0001$) (Table 2).

Longitudinal changes at 2-year follow-up

Next, we re-examined all of the participants after 2 years to address whether the current CT-based HSA detected parameter changes over the 2-year interval. Table 3 summarizes the average values at baseline and the 2-year follow-up for the densitometric and geometrical measurements as well as the biomechanical properties. In each case, the correlations of the changes from the baseline were high, ranging from $r=0.84$ to 0.98 (all; $p<0.0001$).

Importantly, the current CT system detected significant decreases from baseline in total BMD (−0.900 ± 0.257%/year; $p<0.0005$), cortical CSA (−0.800 ± 0.423%/year; $p<0.05$) and cortical thickness (−1.120 ± 0.453%/year; $p<0.01$) at the femoral neck, and also a decrease in the cortical BMD of the femoral shaft (−0.642 ± 0.188%/year; $p<0.005$) (Table 3). These changes in the longitudinal analysis were consistent with the results of the cross-sectional analysis presented above (Table 2).

Our system did not detect any significant changes in the biomechanical properties of the femoral shaft (Table 3). However, a worsening of all the biomechanical properties of the femoral neck the 2-year period was observed; CSMI (−1.38 ± 3.65%/year; $p<0.01$) and SM (−1.37 ± 2.96%/year; $p<0.005$) decreased, and BR increased from the baseline (1.48 ± 4.81%/year; $p<0.05$) (Table 3).

Table 3 also summarizes the results of the longitudinal analysis by comparing the average% changes at the femoral neck versus the shaft. The average% change in cortical BMD was significantly higher in the femoral shaft than in the neck (0.081 ± 0.274%/year, ns in FN, and −0.642 ± 0.188%/year, $p<0.005$ in FS). The average% decreases in the CSMI and SM were significantly greater in the femoral neck (−1.38 ± 3.65%/year, $p<0.01$ for CSMI and −1.37 ± 2.96%/year, $p<0.05$ for SM) than in the shaft (−0.16 ± 2.30%/year, ns for CSMI and −0.32 ± 2.43%/year, ns for SM) (Table 3).

Discussion

It is widely recognized that aging has a substantial impact on the geometry of the proximal femur [4], and data on age-related changes in the hip geometry not only provides crucial insight into the pathogenesis of hip fracture, but also should help form the basis for

Table 3
Longitudinal changes in BMD, geometry and biomechanical properties during the 2-year follow-up.

	Measurement	Unit	Baseline	Follow-up	%change/year	p	p (vs. FS)	Correlations (baseline and follow-up)
FN BMD/geometry								
	Total BMD	mg/cm^3	335.7 ± 58.7	329.8 ± 58.5	−0.900 ± 0.257	<0.0005	-	0.98
	Total CSA	cm^2	5.75 ± 0.74	5.78 ± 0.84	0.417 ± 0.424	ns	-	0.90
	Total bone mass	g	1.89 ± 0.30	1.86 ± 0.28	−0.613 ± 0.390	ns	-	0.92
	Cortical BMD	mg/cm^3	687.9 ± 48.4	688.6 ± 47.7	−0.081 ± 0.274	ns	<0.05	0.84
	Cortical CSA	cm^2	1.96 ± 0.41	1.92 ± 0.37	−0.800 ± 0.423	<0.05	ns	0.94
	Cortical bone mass	g	1.34 ± 0.31	1.32 ± 0.29	−0.776 ± 0.529	ns	-	0.94
	Cortical thickness	mm	1.83 ± 0.40	1.78 ± 0.36	−1.120 ± 0.453	<0.01	-	0.94
	Perimeter	mm	5.78 ± 0.50	5.78 ± 0.56	0.024 ± 0.316	ns	ns	0.88
FS BMD/geometry								
	Cortical BMD	mg/cm^3	1022.6 ± 52.5	1011.5 ± 49.9	−0.642 ± 0.188	<0.005	-	0.86
	Cortical CSA	cm^2	3.58 ± 0.31	3.56 ± 0.32	−0.752 ± 0.499	ns	-	0.97
	Perimeter	mm	8.78 ± 0.48	8.80 ± 0.51	0.114 ± 0.413	ns	-	0.88
Biomechanical property								
FN	CSMI	cm^4	0.613 ± 0.156	0.597 ± 0.159	−1.38 ± 3.65	<0.01	<0.01	0.96
	SM	cm^3	0.448 ± 0.105	0.437 ± 0.108	−1.37 ± 2.96	<0.005	<0.05	0.97
	BR	1	7.06 ± 1.67	7.20 ± 1.61	1.48 ± 4.81	<0.05	-	0.94
FS	CSMI	cm^4	1.304 ± 0.236	1.298 ± 0.231	−0.16 ± 2.30	ns	-	0.96
	SM	cm^3	1.082 ± 0.142	1.075 ± 0.139	−0.32 ± 2.43	ns	-	0.93

Data are shown as mean ± SD. FN, femoral neck; FS, femoral shaft; BMD, bone mineral density; CSA, cross-sectional area; CSMI, cross-sectional moment of inertia; SM, section modulus; BR, buckling ratio; p value, significance in %change/year of parameters; p (vs. FS), significance in %change/year in FN against %change/year in FS; p* value, significance in correlation between baseline and follow-up measurements.

evaluating and understanding the efficacy of intervention. Important questions that remain unanswered include the extent to which age-related geometry changes actually occur, skeletal sites and time scale of these changes, whether they can be detected by non-invasive techniques, and how long an interval is required to demonstrate the clinical efficacy of a certain intervention to prevent or reverse such changes. Practically, since most clinical trials are terminated within 3 years, it is critically important to know whether the effects of any intervention on age-related changes in geometry can be detected non-invasively within the time scale of 2–3 years.

There has been no report to our knowledge on the demonstration of age-related and/or skeletal site-specific changes in the 3D geometry of the proximal femur. The results of our cross-sectional analysis by CT are qualitatively similar to those obtained in a previous DXA-based HSA in a similar population of postmenopausal Japanese women [13]. However, the % changes with aging in the biomechanical parameters such as SM and BR are larger in the current CT-based analysis than in the previous DXA-based study. In this respect, the 3D d_{max} calculation may have contributed to the increased sensitivity to the age-related changes in SM and BR in the current study.

According to the previous DXA-based HSA studies that analyzed the effects of anti-osteoporosis drugs on the geometry [14–16], distinct effects on the femoral neck and shaft were observed. In the current study using non-invasive CT scanning of the proximal femur, all of the biomechanical parameters, CSMI, SM and BR, worsened significantly with advancing age in the femoral neck, while those in the femoral shaft did not change.

The current study using a CT-based system demonstrated that cortical BMD was maintained at a higher level in the femoral shaft than in the femoral neck from the period of early post-menopause through advanced age, and that the decline in cortical BMD was much greater in the femoral shaft than the femoral neck (Table 3). It is counterintuitive that the femoral shaft would maintain a higher BMD throughout this period but nevertheless exhibit a larger bone loss than the femoral neck, since in comparison with the cortex of the femoral shaft [17], the femoral neck is thought to suffer from high cortical porosity. This may reflect a partial volume effect in measuring cortical BMD and thickness by CT, and higher resolution CT or more detailed histological analysis of the cortical bone in femoral neck and shaft may be required to validate the current findings.

The current system did not detect any significant change in the cortical BMD of the femoral neck, but detected changes in cortical thinning at the same site (Table 3). The border between the cortical and cancellous compartments becomes less obvious with aging, and the progression of cortical porosity in the endocortical region makes it difficult to distinguish it from the thinning of the cortex. Due to this limitation inherent in clinical CT, an alteration in cortical thickness, and not cortical bone density, may have been detected as an age-related change. Further efforts to improve the methodology of delineating the border between cortical and trabecular components accurately are thus required.

The findings that the bone perimeter and total CSA in the femoral neck did not change over a 2-year follow-up, while cortical CSA and thickness at the same site decreased significantly, imply that the current CT-based HSA was capable of detecting the progression of endocortical resorption, while the alteration in periosteal apposition rate, at least during this 2-year period, was too small to be detected. Taken together with the results of the cross-sectional analysis at baseline that both the bone perimeter and total CSA in the femoral neck correlated positively with age, a longer follow-up period would allow a determination of whether the periosteal bone formation continues at a slow pace.

In conclusion, the data presented in this study on age-related alterations in the geometry and biomechanical properties at distinct sites of the proximal femur should provide a basis for an improved understanding the pathogenesis of fracture, and also serve as a foundation for the design of new anti-fracture remedies in postmenopausal women.

Acknowledgments

The authors thank Toru Fukuda and Takako Shimogama (Division of Radiology, Nagasaki University Hospital) for technical assistance and Dr. Kyoji Ikeda (Department of Bone and Joint Disease, National Center for Geriatrics and Gerontology, Obu, Aichi, Japan) for comments on the manuscript. This study was supported in part by a grant for the Promotion of Fundamental Studies in Health Sciences of the National Institute of Biomedical Innovation (NIBIO) of Japan (06-31 to MI) and a Grant-in Aid for Scientific Research in Japan (22591344 to MI). Pacific Edit reviewed the manuscript before submission.

References

[1] Rivadeneira F, Zillikens MC, De Laet CEDH, Hofman A, Uitterlinden AG, Beck TJ, et al. Femoral neck BMD is a strong predictor of hip fracture susceptibility in elderly men and women because it detects cortical bone instability: The Rotterdam Stud. J Bone Miner Res 2007;22:1781–90.
[2] Kaptoge S, Beck TJ, Reeve J, Stone KL, Hillier TA, Cauley JA, et al. Prediction of incident hip fracture risk by femur geometry variables measured by hip structural analysis in the study of osteoporotic fractures. J Bone Mier Res 2008;23:1892–904.
[3] Ito M, Wakao N, Hida T, Matsui Y, Abe Y, Aoyagi K, et al. Analysis of hip geometry by clinical CT for the assessment of hip fracture risk in elderly Japanese women. Bone 2010;46:453–7.
[4] Seeman E, Delmas PD. Bone quality-the material and structural basis of bone strength and fragility. N Engl J Med 2006;354:2250–61.
[5] Sigurdsson G, Aspelund T, Chang M, Jonsdottir B, Sigurdsson S, Eiriksdottir G, et al. Increasing sex difference in bone strength in old age: The age, gene/environment susceptibility-reykjavik study (AGES-REYKJAVIK). Bone 2006;39:644–51.
[6] Riggs BL, Melton LJ, Robb RA, Camp JJ, Atkinson EJ, Peterson JM, et al. Population-based study of age and sex differences in bone volumetric density, size, geometry, and structure at different skeletal sites. J Bone Miner Res 2004;19:1945–54.
[7] Takada J, Beck TJ, Iba K, Yamashita T. Structural trends in the aging proximal femur in Japanese postmenopausal women. Bone 2007;41:97–102.
[8] Ito M, Nishida A, Kono J, Kono M, Uetani M, Hayashi K. Which bone densitometry and which skeletal site are clinically useful for monitoring bone mass? Osteoporos Int 2003;14:959–64.
[9] Orimo H, Hayashi Y, Fukunaga M, Sone T, Fujiwara S, Shiraki M, et al. Osteoporosis Diagnostic Criteria Review Committee: Japanese Society for Bone and Mineral Research. Diagnostic criteria for primary osteoporosis: year 2000 revision. J Bone Miner Metab 2001;19:331–7.
[10] Genent HK, Wu CY, van Kuijk C, Nevitt MC. Vertebral fracture assessment using a semiquantitative technique. J Bone Miner Res 1993;8:1137–48.
[11] Power J, Loveridge N, Lyon A, Rushton N, Parker M, Reeve J. Bone remodeling at the endocortical surface of the human femoral neck: a mechanism for regional cortical thinning in cases of hip fracture. J Bone Miner Res 2003;18:1775–80.
[12] Kaptoge S, Beck TJ, Reeve J, Stone KL, Hiller TA, Cauley JA, et al. Prediction of incident hip fracture risk by femur geometry variables measured by hip structural analysis in the study of osteoporotic fractures. J Bone Miner Res 2008;23:1892–904.
[13] Takada J, Beck TJ, Iba K, Yamashita T. Structural trends in the aging proximal femur in Japanese postmenopausal women. Bone 2007;41:97–102.
[14] Uusi-Rasi K, Semanick LM, Zanchetta JR, Bogado CE, Eriksen EF, Sato M, et al. Effects of teriparatide [rhPTH (1-34)] treatment on structural geometry of the proximal femur in elderly osteoporotic women. Bone 2005;36:948–58.
[15] Bonnick SL, Beck TJ, Cosman F, Hochberg MC, Wang H, de Papp AE. DXA-based hip structural analysis of once-weekly bisphosphonate-treated postmenopausal women with low bone mass. Osteoporos Int 2009;20:911–21.
[16] Ito M, Sone T, Fukunaga M. Effect of minodronic acid hydrate on hip geometry in Japanese women postmenopausal osteoporosis. J Bone Miner Metab 2010;28:334–41.
[17] Bousson V, Meunier A, Bergot C, Vicaut E, Rocha MA, Morais MH, et al. Distribution of intracortical porosity in human midfemoral cortex by age and gender. J Bone Miner Res 2001;16:1308–17.

CTによる骨質評価と骨折リスク

伊東　昌子*

Evaluation of Bone Quality and Fracture Risk Using Clinical CT

Masako Ito

臨整外 45：881～886，2010

Key words：コンピュータ断層撮影法(computed tomography)，骨ジオメトリー(bone geometry)，骨微細構造(microstructure)

CTによる骨質評価は構造特性の評価であり，骨ジオメトリーと海綿骨微細構造解析によって，骨折リスク予測や薬物効果評価に用いられるようになってきた．通常のCTが断面画像であるのに対して，多列検出器を有するmulti detector-row CT(MDCT)は容積画像を提供するので，三次元データに基づいて任意の断面での再構成画像を得ることができる．また高い空間分解能を提供するため，海綿骨微細構造解析の臨床における有用性も確認され，研究が進められている．今後テクノロジーの進歩による実用化を期待する．

はじめに

骨折リスクは骨密度のみで十分説明できないこと，また骨密度による薬効評価は感度が低いことが知られており，骨密度とともに骨質も考慮した骨評価が望まれている．しかしながら，現在臨床における骨質評価法はまだ十分に確立されていない．

X線computed tomography(CT)による骨質評価は構造特性の評価であり，骨ジオメトリーと海綿骨微細構造評価に用いられている．CTが骨構造描出に優れているのは，高い空間分解能と密度分解能を有し，三次元データを提供する点にある．

X線CT装置と骨解析

X線CTスキャナはX線照射した目的部分のX線減弱係数値の分布をコンピュータで算出して，多方向からの投影データをもとに内部構造を再構成したものである(図1)．

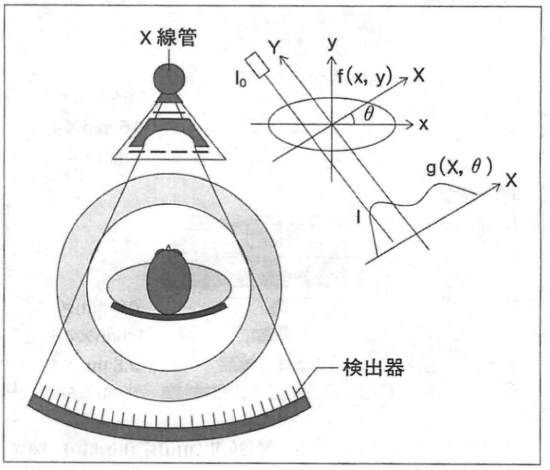

図1　CT(computed tomography；コンピュータ断層撮影法)の原理
CTの投影データはX線管球から照射され被写体を透過して減衰を受けたX線を検出器で測定した強度として与えられる．
上図のように被写体に固定した座標上で，被写体の線減弱係数の分布f(x，y)を求める．

多列検出器をもつCT装置は，multi detector-row CT(MDCT，図2)と呼ばれ，通常のCTが断面画像であるのに対して，MDCTは容積画像を

* 長崎大学病院放射線部〔〒852-8501 長崎市坂本1-7-1〕Department of Radiology, Nagasaki University Hospital

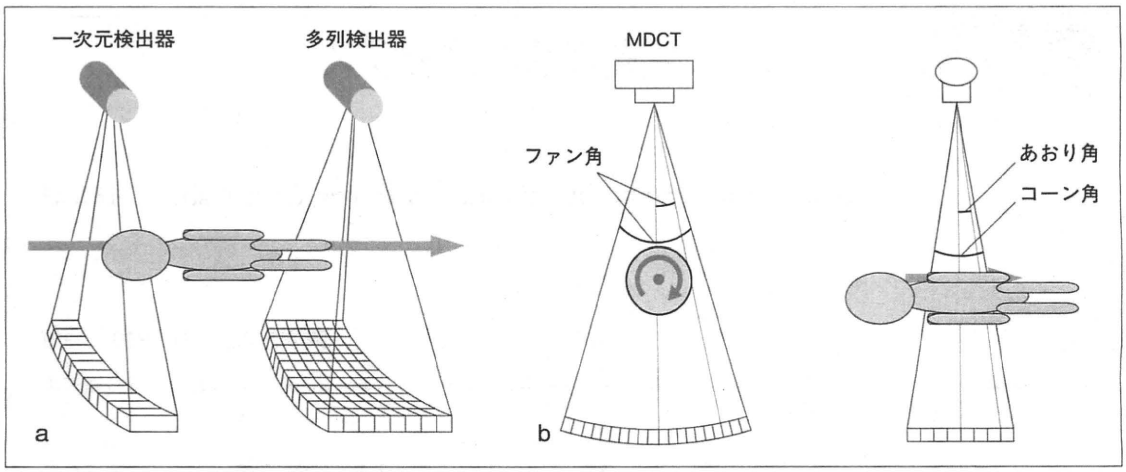

図2　MDCT(multi detector-row CT)とシングルスライス CT

a：シングルスライス CT は検出器が XY 平面に並び，Z 軸方向には 1 列である．Z 軸方向に検出器を多列にしたのが MDCT である．

b：MDCT の検出器は，XY 平面では，X 線管を中心にして配列している．Z 方向では平面に並ぶ．

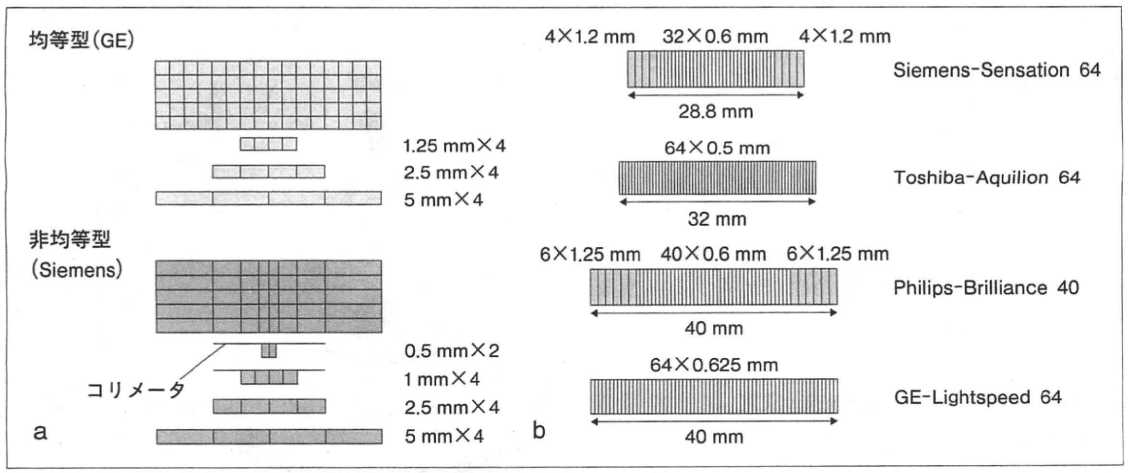

図3　MDCT(multi detector-row CT)と DAS(data acquisition system)

a：実際のスキャンでは多列検出器のうちの同時収集可能列数を選択して，DAS(data acquisition system；データ収集装置)で束ねて出力する．つまり，DAS によってスライス厚が異なる．例えば検出器の配列が均等型の場合では，1.25 mm の 4 列をデータ収集に使用する場合，2.5 mm の 4 列をデータ収集に使用する場合，5 mm の 4 列をデータ収集に使用する場合で，スライス厚が異なり分解能は異なる．

b：装置によって検出器の配列は均等型と非均等型がある．

提供するので，①高速スキャン，②広範囲の撮影，③薄いスライスの画像データ(thin slice data)を可能とした(図 3)．骨解析には循環器系の検査のような高速スキャンは要求されないが，骨評価における MDCT の有用な点は，①高い空間分解能を提供できる，②三次元データに基づいて，任意の断面での再構成画像を得ることである．図 3 に示すように DAS(data acquisition system)により，スライス厚やスキャン範囲と速度を調節できる．

Magnetic resonance(MR)も同様に三次元データを得ることができるが，皮質骨に関してのデータが得られないこと，撮像に時間がかかることなどの問題点がある．

海綿骨梁構造は棒状と板状の骨梁が連結しあって構成され，個々の骨梁の幅は 50〜200 ミクロン，

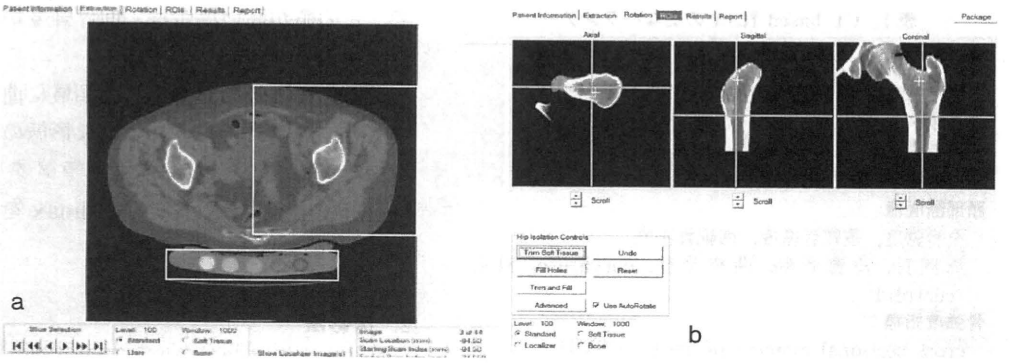

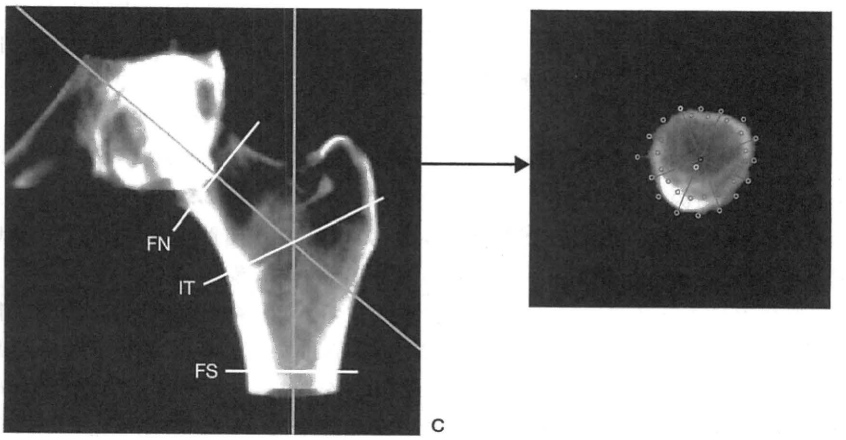

図4　CT-based HSA の概要
a：骨量ファントムを被験者背側において，大腿骨近位部をスキャンする．
b：大腿骨頚部長軸，骨幹部長軸(矢状断，冠状断)を抽出し，大腿骨近位部のオリエンテーションを定める．
c：大腿骨頚部(FN，最狭部)，転子部(IT)，骨幹部(FS)
骨密度測定領域と頚部横断面像．

骨梁間距離は200～1,000ミクロンである．骨梁構造評価の目的は，骨強度予測，骨病態解明および薬効評価が挙げられ，これらの目的のために，摘出骨サンプルを対象にマイクロCTが用いられるが，*in vivo* 検査としてのMDCTは高分解能画像を提供するものの，マイクロCTレベルの分解能を得ることは不可能である．つまりCTのボクセル(三次元空間での正規格子単位の体積の値)サイズよりも小さいサイズの骨梁を描出することとなり，部分容積効果(partial volume effect)によって，真の骨梁構造としての可視化・定量化は困難である．部分容積効果とは，隣接する2つの臓器の境界面がスライス面に対して斜めに存在したり，小さな組織の場合に，異なった組織のCT値がボクセル内で平均化され境界が不鮮明となる現象のことである．

臨床用CTを用いた骨ジオメトリー評価

1. CT-based hip structure analysis(HSA)の概要

大腿骨近位部dual X-ray absorptiomery(DXA)データに基づき，非侵襲的にジオメトリーと骨強度指標を算出するhip structure analysis(HSA)[1]をDXA-based HSAと呼ぶのに対して，X線CTを用いた大腿骨の骨ジオメトリー解析はCT-based HSA(図4)と呼ばれる．DXA-based HSAでは，DXA測定値を一定のアルゴリズムで三次元データに概算する方法であるので，あくまでも骨密度に依存するジオメトリーであるという問題点がある[10]．

一方，CTでは骨密度から独立した形態を評価できる利点がある．また，三次元データに基づき任意断面像を得ることができるので，頚部軸を三次元的に検出し，さらに頚部長軸を基準に頚部横

表1　CT-based HSA の主なパラメター

骨密度
面積密度・容積密度(頚部，転子部，骨幹部)
骨ジオメトリー
大腿骨頚部長(hip axis length：HAL)
頚体角(neck shaft angle)，大腿骨頚部幅
頚部断面像
全骨密度，皮質骨密度，海綿骨密度
周囲長，皮質骨幅，曲率半径，curvature，重心(centroid)
骨強度指標：
cross-sectional moment of inertia(CSMI)
section modulus(SM)
buckling ratio(BR)

断面から皮質骨幅や皮質骨周囲長などを求めて骨強度指標を算出できる．

CT-based HSA には，市販の QCT PRO(Mindways 社製)のほか，自家製ソフトウェア[3-4]が使用されている．CT-based HSA で得られるパラメターを表1，図5に示す．

骨強度パラメターについて簡単に説明する．Cross-sectional moment of inertia(CSMI)は曲げモーメントに対する物体の変形のしにくさを表した量であり，断面の微小面積要素と，その箇所の X 軸からの距離の2乗の積の総和である．

Section modulus(SM)とは，CSMI を骨量中心からの最大外径(dmax)で除して算出されたもので，この値が高い場合は，曲げ強度が高いことを意味する．

また，皮質骨の菲薄化した領域に曲げの外力が働くと，内側に折れ込むような形態の骨折(座屈)を引き起こす．その骨強度パラメターは座屈比 buckling ratio(BR)であり，dmax を平均皮質骨幅(CoTh)で除した値である．

2. 撮影法

使用する装置に適合した撮像条件の設定が必要であるが，標準的な日本人の体型では，120 KVp，250～300 mAs，500～1,000 ミクロンスライス厚でのデータ収集が適していると考えている．ビームピッチは1未満として，スライス間のつなぎ目を滑らかにすることが必要である．骨密度測定を行うため，また，データ解析における二値化の閾値を決定するため，骨密度測定用校正ファントムを用いる．アーチファクトが生じないように，人体とファントムの間に緩衝バッグを補填するのがよい．CT 装置は quality control(QC)を行って，エネルギー出力を安定させた状態でスキャンできるようにする．また，CT テーブルの高さは一定として同じ条件(KVp，mAs，ビームピッチ)でスキャンし，同じ再構成フィルターを用いる．再構成フィルターは画像診断用骨イメージ用よりもや

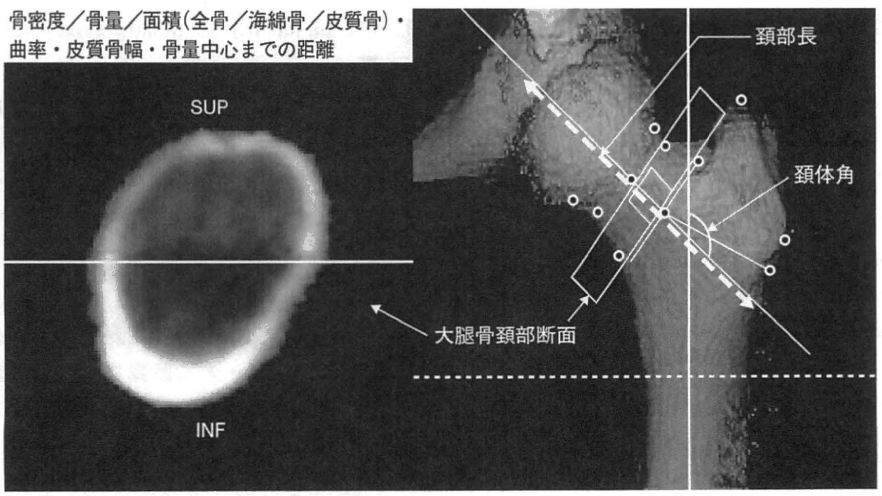

図5　CT-based HSA で得られる主なパラメター
頚部長軸に直交する大腿骨頚部横断面像を得て，その画像から，全骨・皮質骨・海綿骨の骨密度・骨量・面積，ならびに曲率，皮質骨幅・骨量中心までの距離を算出する
SUP：上，INF：下

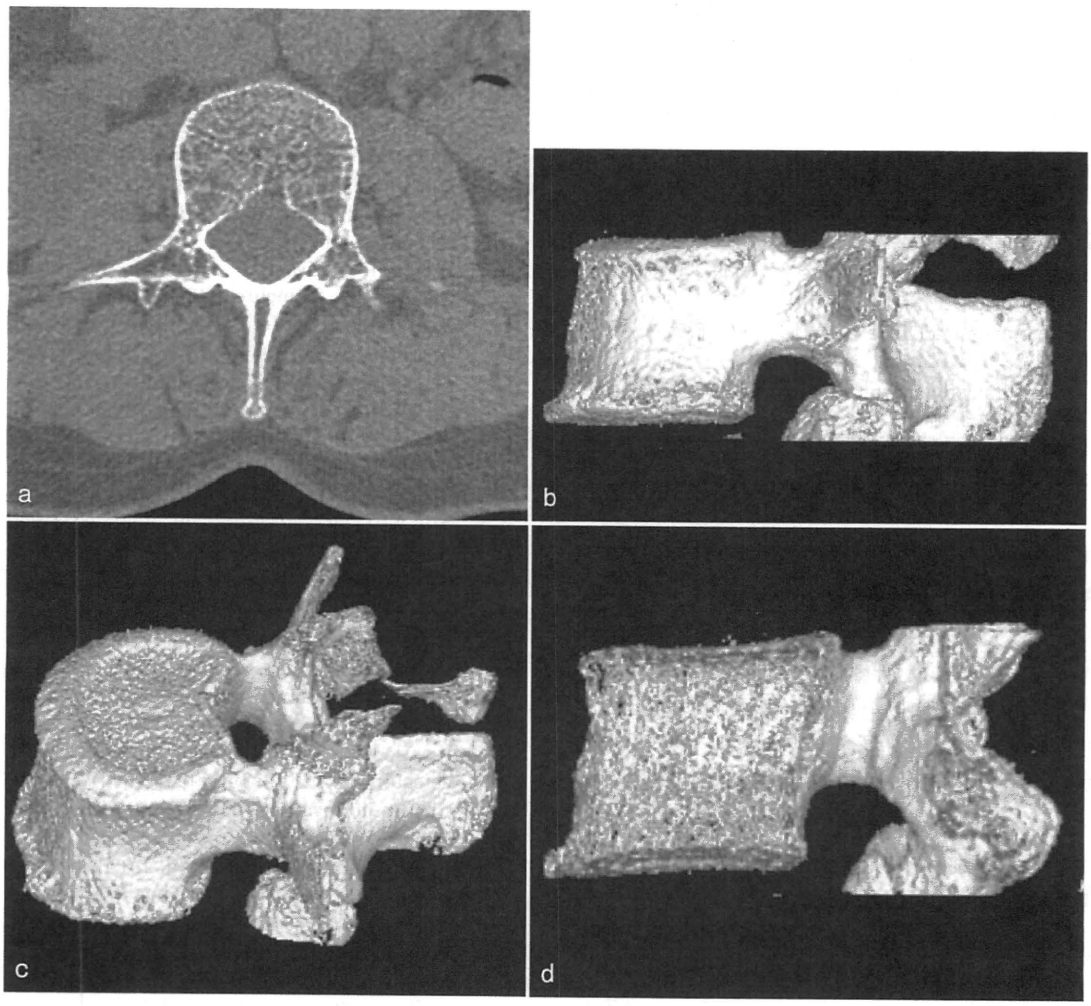

図6　ヒト椎体の MDCT 画像
a：二次元オリジナル画像　　**b**，**c**：三次元再構成画像　　**d**：c の矢状断割面（微細構造を描出）

やコントラストが弱いほうがよい．

3. CT-based HSA による骨折リスク評価

屍体大腿骨を高解像度 peripheral QCT で解析した研究[8]では，大腿骨頚部において上背側では荷重の影響が少ないため，同部の皮質骨幅は加齢に伴い菲薄化するが，その変化は骨脆弱性と関連していることが報告されている．われわれは，臨床用 CT を用いて大腿骨頚部骨折と転子部骨折の骨折におけるジオメトリーの特徴を検討[6]したが，頚部骨折においては大腿骨頚部長 hip axis length（HAL）が有意に長く，CSMI が有意に低く，BR が有意に高かった．また，転子部骨折においては大腿骨頚部の皮質面積が有意に小さいことがわかった．

4. CT-based HSA による薬効評価

テリパラチドの薬効を CT-based HSA を用いて評価した 24 カ月の前向き試験において，大腿骨頚部の皮質骨密度は減少したが，断面積が増加し，BR を改善したことが報告されている[2]．

MDCT を用いた骨梁構造解析

躯幹骨は末梢骨よりも骨折リスクの評価に感度が高いので，脊椎骨梁構造を評価する意義は大き

表2　骨微細構造の主なパラメター

骨形態計測学的パラメター
骨組織容積比　bone volume(BV)/total tissue volume(TV)(%)
骨梁幅　Tb.Th(mm)
骨梁間距離　Tb.Sp(mm)
骨梁数　Tb.N(1/mm)
空間的構造を表すパラメター
degree of anisotropy(DA)：異方性度：骨梁の方向性を定量化したパラメター
structure model index(SMI)：骨梁の形態を定量化するパラメター
trabecular bone pattern factor(TBPf)：骨梁表面の凹凸形態を評価するパラメター
connectivity density：連結密度：骨梁連結性の定量化を表すパラメター

い．われわれはMDCTを用いて，腰椎海綿骨梁構造を三次元的に可視化(図6)し，構造パラメターを算出して臨床的有用性を検討した[5]．その結果，MDCTで算出した骨梁構造パラメターは，DXAで測定する骨密度以上に骨折リスクを予知できることが考えられた．主な骨微細構造パラメターを表2に示す[4]．また，骨粗鬆症治療薬の効果評価としても，臨床用CTを用いた海綿骨微細構造解析が行われ，薬物の効果メカニズム解明に貢献する結果が報告されている[3]．

高い解像度を得るにはX線被曝量が高くなることは十分理解して適用を考える必要がある．テクノロジーの進歩によって，一般臨床への応用が可能になることを期待したい．

有限要素解析 finite element analysis(FEA)への応用

CTの三次元骨梁構造データ，あるいは個々のボクセルのCT値から換算した骨密度分布データに基づく有限要素解析で，骨の力学特性を評価することができる．詳細は次稿「定量的CTを用いた有限要素法による骨強度評価」を参照いただきたい．

文　献

1) Beck TJ, Looker AC, Ruff CB, et al : Structural trends in the aging femoral neck and proximal shaft : analysis of the third national health and nutrition examination survey dural-energy X-ray absorptiometry data. J Bone Miner Res **15** : 2297-2304, 2000
2) Borggrefe J, Graeff C, Nickelsen TN, et al : Quantitative computed tomographic assessment of the effects of 24 months of teriparatide treatment on 3-D femoral neck bone distribution, geometry and bone strength : Results from the EUROFORS study. J Bone Miner Res **25** : 472-481, 2010
3) Graeff C, Timm W, Nickelsen TN, et al : Monitoring teriparatide associated changes in vertebral microstructure by high-resolution computed tomography *in vivo*. Results from the EUROFORS study. J Bone Miner Res **22** : 1426-1433, 2007
4) Hildebrand T, Ruegsegger P : A new method for the model independent assessment of thickness in three-dimensional images. J Microsc **185** : 67-75, 1997
5) Ito M, Ikeda K, Nishiguchi M, et al : Multi-detector row CT imaging of vertebral microstructure for evaluation of fracture risk. J Bone Miner Res **20** : 1828-1836, 2005
6) Ito M, Wakao N, Hida T, et al : Analysis of hip geometry by clinical CT for the assessment of hip fracture risk in elderly Japanese women. Bone **46** : 453-457, 2010
7) Kang Y, Engelke K, Fuchs C, et al : An anatomic coordinate system of the femoral neck for highly reproducible BMD measurements using 3D QCT. Compt Med Image Graph **29** : 533-541, 2005
8) Mayhew P, Thomas CD, Clement JG, et al : Relation between age, femoral neck cortical stability, and hip fracture risk. Lancet **366** : 129-135, 2005
9) Meta M, Lu Y, Keyak JH, et al : Young-elderly differences in bone density, geometry and strength indices depend on proximal femur sub-region : A cross sectional study in Caucasian-American women. Bone **39** : 152-158, 2006
10) Szulc P, Duboeuf F, Schott AM, et al : Structural determinants of hip fracture in elderly women : re-analysis of the data from the EPIDOS study. Osteoporos Int **17** : 231-236, 2006

3 骨粗鬆症における骨構造の変化

■伊東昌子（いとうまさこ）
長崎大学病院 放射線部

伊東 昌子
長崎県出身。長崎大学医学部卒業。専門は放射線医学と骨粗鬆症。研究テーマは画像を用いた骨解析，骨質評価。

Key words：microstructure，geometry，bone strength，computed tomography

Abstract
骨粗鬆症における海綿骨の微細構造変化の特徴は，骨体積比の減少，骨梁連結性低下，骨梁形態の板状から棒状への変化，骨梁間距離の増加，骨梁数の減少であり，皮質骨微細構造では皮質骨多孔化とそれに関連したマクロクラックの発生・進展がある。長管骨横断面ジオメトリーの特徴は，内膜側骨吸収による骨髄腔の拡大と，皮質骨幅減少，皮質骨多孔化による皮質骨密度の減少，外膜側での骨面積の拡大がみられる。このような骨粗鬆症における骨構造の変化は，加齢変化の延長上の変化であり，脆弱性骨折の原因の一つとなる。

はじめに

2000年にNational Institute of Health（NIH; 国立衛生研究所）が発表した定義によると，骨粗鬆症は骨強度の低下によって骨折リスクが高くなる骨の疾患であり，骨強度には骨密度と骨質の両方が関与するとしている。

骨質に属する構造特性と材質特性のうち，本章では，骨粗鬆症における構造特性の変化，つまり海綿骨と皮質骨微細構造，ならびに骨ジオメトリーの変化を骨強度との関連を視野において述べる。

1．骨粗鬆症と海綿骨微細構造

骨粗鬆症における海綿骨の構造変化の特徴は，骨体積比の減少，骨梁連結性の低下，骨梁形態の板状（plate-like）から棒状（rod-like）への変化，骨梁間距離の増加，骨梁数の減少である（図1）。エストロゲン欠乏状態において観察される局所的な骨梁表面の深い骨吸収（吸収窩）が発生した場合でも，局所的な骨梁幅の菲薄化と骨梁連結性の断裂をひきおこすが，平均骨梁幅は比較的維持されるため，骨梁幅の減少として捉えられないことがある。一方，グルココルチコイド誘発性骨粗鬆症では，深い吸収窩はあまり形成されず，全体的に骨梁幅が菲薄化するので，骨梁連結性の断裂よりも骨梁幅の減少が特徴だと考えられている。加齢や骨粗鬆化では，板状の骨梁が棒状の骨梁形態に変化するのは，板状骨梁に吸収窩が生じて，それが拡大したことによる変化である。また，異方性度に関しては，荷重負荷の存在下では，少ない骨量で強度を維持するために荷重負荷の高い骨梁を残存させて，その幅を太くするメカニズムが働き，そのた

Bone structure in osteoporosis：Masako Ito, Division of Radiology,Nagasaki University Hospital

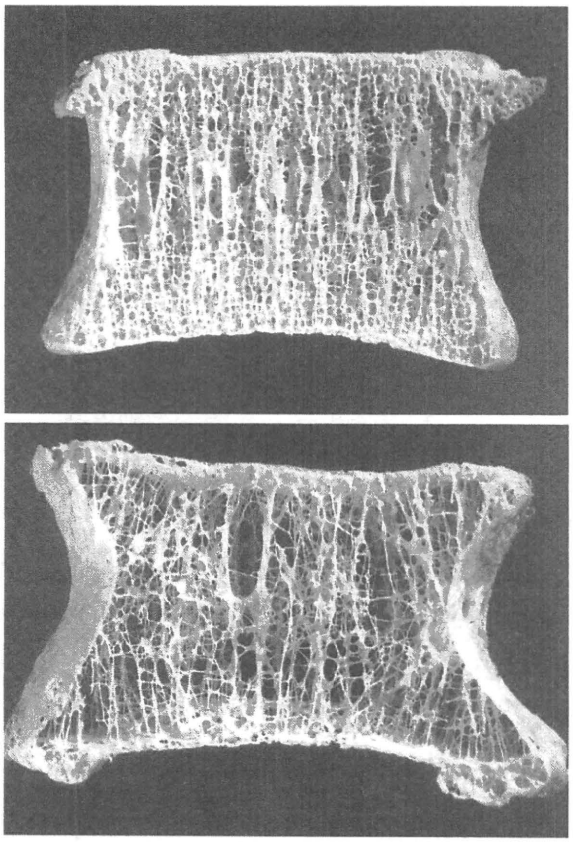

図2　健常な海綿骨骨梁構造（上図）と骨粗鬆症の骨梁構造（下図）。骨粗鬆症では，骨梁が細く粗になり連結性が低下しているが，骨梁の方向や太さが変わり，荷重に耐えられるように適合している状態が示される
Mosekilde L.Z Rheumatol59,2000より引用

いて横走・縦走する骨梁の分布パターンを認識して，骨の粗鬆化を判定する方法である。

大腿骨近位部に認められる骨梁群は，主抗圧骨梁群，副抗圧骨梁群，大転子部骨梁群，主抗張骨梁群，副抗張骨梁群があり，骨粗鬆症においては，主抗圧骨梁群の骨吸収が他の骨梁群に比べ少ないことがX線像で認識されている。それは，この骨梁群は荷重負荷が大きく，その維持が身体を支えるのに重要な骨梁群だからである。また，大腿骨頸部骨折を発生した患者においては，対照群に比べて大腿骨頸部の主抗圧骨梁群に対して垂直方向に走行する骨梁の消失が目立つと報告されている[3]。このような所見に基づき，Singhの分類は大腿骨近位部の骨梁群の変化を，X線像で骨粗鬆化の程度として6段階に分類したものである[4]。

2．骨粗鬆症と皮質骨微細構造

骨粗鬆症における皮質骨の構造変化の特徴には，皮質骨幅の菲薄化と皮質骨の多孔化がある。

皮質骨微細構造は高い解像度を有するシンクロトロンCTや組織像で評価される。皮質骨に認められる小腔は血管腔と骨細胞小腔からなり，骨粗鬆化では血管孔や骨細胞小胞が増加拡大する。マイクロクラックは血管孔の辺縁より発生しやすく，骨細胞小胞を貫通しながら隣の骨細胞小胞に向かって進展する[5]。シンクロトロンCTでは，三次元的視覚化が可能であるので，血管腔と骨細胞小腔およびマイクロクラックのそれぞれの関係を三次元的に評価して，マイクロクラックの進展の様式をとらえようとしている。

皮質骨外膜側・中央・内膜側の3部位に分けて，多孔化を比較すると，①男性・女性とも加齢に伴い多孔率が増加，とくに閉経後女性で顕著　②外膜側よりも中央，中央よりも内膜側において多孔性の増加が顕著　③高齢女性においては内膜側の多孔化は顕著で，そ

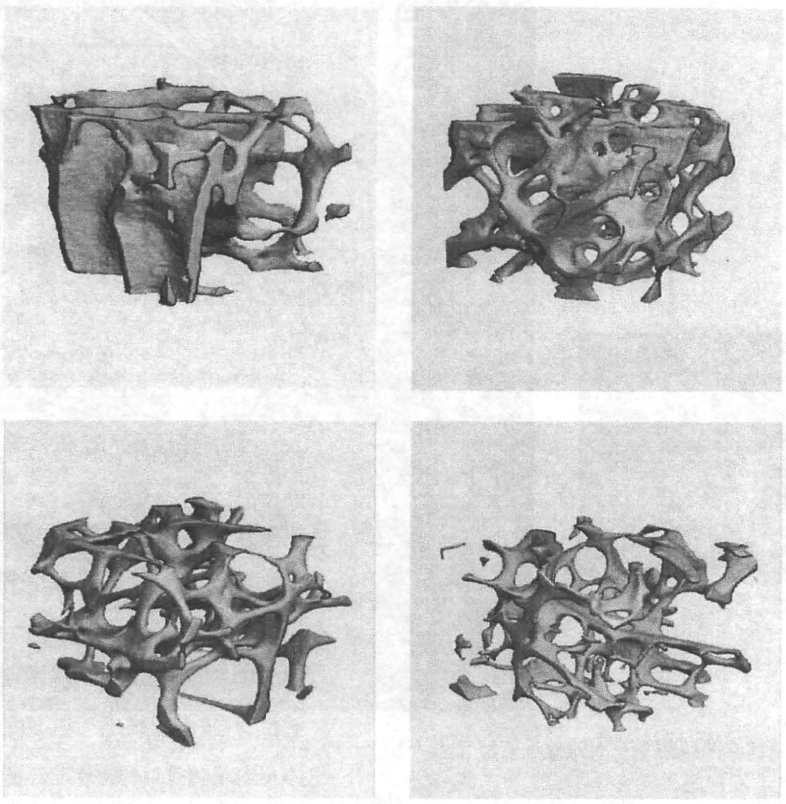

図1 骨粗鬆症における海綿骨骨梁構造。骨梁の形態は板状骨梁が棒状骨梁に変化（左図）し，連結性が低下（右図）する。骨量の減少，骨量数の減少，骨梁間距離の増加などの特徴も見られる。右上図，主に板状骨梁からなる構造。左下図主に棒状骨梁からなる構造。右上図，骨梁連結性が良好な構造。右下図，連結性が低下した構造。

め異方性度は上昇する。骨量の減少した骨粗鬆症の椎体では，少ない材量（骨量）で荷重に対抗できるような骨梁分布を示しているのが観察される（**図2**）。したがって非荷重の状態で骨減少が生じる場合では，この現象は観察されない[1]。

海綿骨骨梁構造は，骨の部位によって特徴が異なり，骨粗鬆症における変化も部位によって異なることが知られている[2]。骨梁構造の加齢変化や骨粗鬆症化のパターンがよく知られている，椎体と大腿骨近位部について述べる。

椎体には，主として縦方向と横方向に走行する骨梁が連結して存在する。骨粗鬆症の椎体では，荷重方向に垂直に走行する横方向の骨梁が菲薄化・断裂，あるいは消失するが，縦方向の骨梁は相対的に残存し，さらに縦方向の骨梁では加齢とともに幅が増大する場合（異方性の増大を意味する）も観察される。慈大式骨萎縮度分類は，椎体側面X線像にお

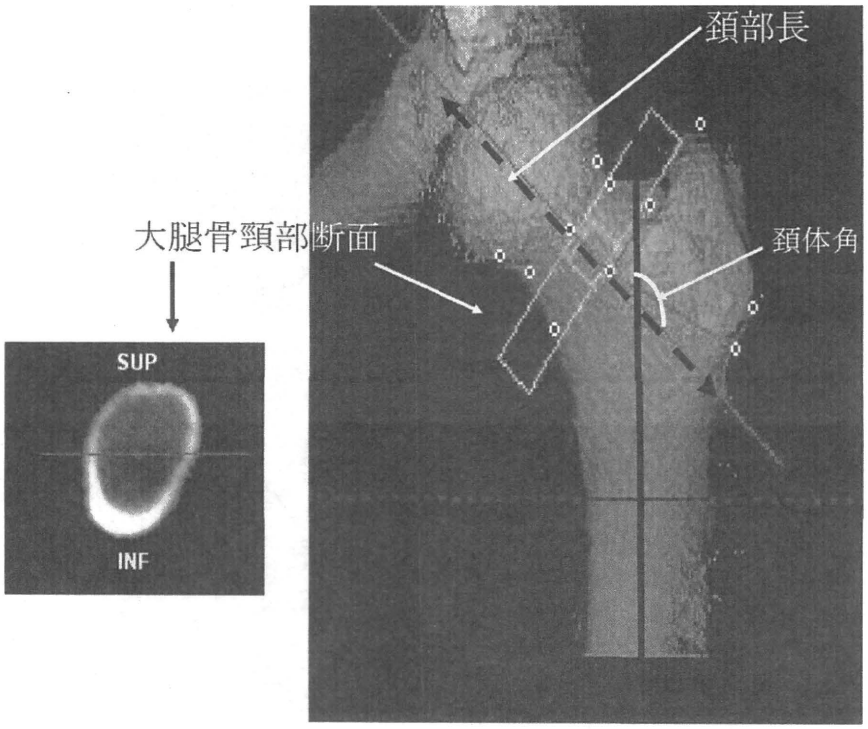

図4　CT画像に基づく大腿骨近位部ジオメトリーの評価法。頸部長軸に直交する大腿骨頸部横断面像を得て，その画像より，全骨・皮質骨・海綿骨の骨密度・骨量・面積，ならびに曲率，皮質骨幅・重心までの距離を算出する。これらのジオメトリーの結果に基づき，強度指標　CSMI:断面二次モーメント（曲げ強度の指標），BR:buckling ratio（cortical stabilityの指標）を算出する。

すると，大腿骨頸部において上背側では荷重を強く受けないため，同部位では皮質骨密度は他の部位より低く，皮質骨幅は加齢に伴って著しく菲薄化することが報告されている。一部で頸部の前面部の皮質骨幅は加齢に伴って増大し，これらの変化に伴って大腿骨頸部の重心が下方へ偏位するため，皮質骨不安定性が強くなると考えられる。図3は，縦断的に経過をみたものではないが，大腿骨頸部横断面の加齢変化の特徴を示したCT画像である。

臨床用X線CTを用いて大腿骨近位部ジオメトリー解析を行う方法は，CT-based hip structure analysis （HSA）と呼ばれている。CT-based HSAでは三次元データに基づくため頸部軸や骨幹軸の描出，さらに頸部軸を基準に頸部横断面像を求めることができる点が優れており，長管骨の横断面CT像より全骨面積，皮質骨面積，外径，外周囲長の計測が可能であり，それに基づき骨強度パラメターを求めることもできる（図4）。骨粗鬆症における長管骨ジオメトリーの変化の特徴は，皮質骨面積の減少，皮質骨幅の減少（不均等減少），内径・外周囲長の増加である。